Clim. Past Discuss., 11, 3187–3209, 2015
www.clim-past-discuss.net/11/3187/2015/
doi:10.5194/cpd-11-3187-2015

Climate of the Past
Discussions
Open Access

Holocene climate variability in the North-Western Mediterranean Sea (Gulf of Lions)

B. Jalali[1,2], M.-A. Sicre[2], M.-A. Bassetti[3], and N. Kallel[1]

[1]GEOGLOB, Université de Sfax, Faculté des Sciences de Sfax, route de Soukara km 4-BP.802, 3038, Sfax, Tunisia
[2]Sorbonne Universités (UPMC, Université Paris 06)-CNRS-IRD-MNHN, LOCEAN Laboratory, 4 place Jussieu, 75005 Paris, France
[3]CEFREM, Université de Perpignan, Avenue J.-P. Alduy, 66860 Perpignan, France

Received: 11 June 2015 – Accepted: 24 June 2015 – Published: 16 July 2015

Correspondence to: B. Jalali (bassemjalali@yahoo.fr)

Published by Copernicus Publications on behalf of the European Geosciences Union.

CPD
11, 3187–3209, 2015

Abstract

Sea surface temperatures (SSTs) and land-derived input time series were generated from the Gulf of Lions inner-shelf sediments (NW Mediterranean Sea) using alkenones and high-molecular-weight odd-carbon numbered *n*-alkanes (TERR-alkanes), respectively. The SST record depicts three main phases: a warm Early Holocene (∼ 18 ± 0.4 °C) followed by a cooling of ∼ 3 °C (from 7000 to 1000 BP) and rapid warming from ∼ 1850 AD onwards. Several superimposed multi-decadal cooling events of ∼ 1 °C amplitude were also identified. TERR-alkanes were also quantified to identify periods of high river discharge in relation with flood events of the Rhone River and precipitations. Their concentrations show a broad increase from the early Holocene towards present with a pronounced minimum around 2500 BP and large fluctuations during the second part of the Holocene. Comparison with Holocene flood activity reconstructions across the Alps region suggests that sediments of the inner shelf originate mainly from the Upper Rhone River catchment basin and that they are primarily delivered during positive NAO.

1 Introduction

Several proxy records have documented surface water variability of the Mediterranean Sea during the Holocene (Cacho et al., 2001; Guinta et al., 2001; Rohling et al., 2002; Emeis et al., 2003; Essalami et al., 2007; Frigola et al., 2007; Castaneda et al., 2010; Martrat et al., 2014). Most of them reveal that Sea surface temperatures (SSTs) have undergone a long-term cooling punctuated by several cold relapses (CR) (Cacho et al., 2001; Frigola et al., 2007). While orbital forcing likely accounts for the temperature long-term trend, solar activity and volcanism have been proposed to be partly responsible for the multi-decadal variability (Mayewski et al., 2004; Wanner et al., 2011). Modes of internal variability (i.e. Atlantic Multi-decadal variability (AMV), North Atlantic Oscillation (NAO)...) are also embedded in decadal-scale variations in paleo time-series, but difficult to decipher in climate (internal) variability. Because of strong ocean/atmospheric interactions in the Mediterranean region, changes in the large-scale atmospheric circulation pattern are expected to impact on the high frequency component of the paleo-SST signal. Josey et al. (2011) have shown that the East Atlantic pattern (EA) and the NAO are the most important modes of atmospheric variability influencing heat loss and thus convection in areas of deep-water convection of the Mediterranean. Notably, it has been shown that episodes of deeper convection in winter 2004/05 and 2005/06 in the Gulf of Lions were triggered by intense winds closely related to negative EA and NAO (Schroeder et al., 2011).

In this study, we produced a high-resolution SST record of the past 10 000 yr based on the alkenones to document changes in the Gulf of Lions and their link with atmospheric circulation. TERR-alkanes were determined in the same sediment horizons to assess land-derived inputs from the Rhone River plume, in an attempt to identify flood periods in its catchment basin and link them to the long-term precipitation variability in the Western Mediterranean basin.

2 Materiel and methods

2.1 Oceanographic setting and sampling

Surface circulation in the Gulf of Lions is characterized by the geostrophic North Current of 30 to 50 km width flowing along the continental slope from the Ligurian to the Catalan basins (Millot, 1990). This current is highly variable and has a strong mesoscale activity (eddies and meanders) that impact on the renewal of the surface waters (Millot, 1999). Along its path, the North Current receives freshwater and suspended matter mostly from the Rhone River. In the inner shelf, the westward coastal flow is able to advect the river plume suspended particles settling as a wedge-shaped body, defined as mud belt (Cattaneo et al., 2003; Bassetti et al., 2015).

Annual SSTs in the Gulf of Lions are colder than mean annual values for the whole Mediterranean basin owing to the strong vertical mixing caused by intense winter storms associated with cold and dry continental winds blowing in this area, i.e. Mistral and Tramontane (Fig. 1). The Tramontane originates from the northwest blowing through the Naurouze passage, while Mistral winds are northerly winds channeled by the Rhone river valley (Auclair et al., 2000). Dense waters are thus formed during winter upon cooling and evaporation and then spread to the bottom floor over the continental shelf down to the abyssal plain. However, the heat and salt contents of the underlying Levantine Intermediate waters (LIW) can affect the near surface water buoyancy and thus deep-water formation (Schroeder et al., 2011).

Rainfall in the NW Mediterranean Sea mainly occurs during winter (October to March). It is very dependent on the storm tracks position and intensity of the winter NAO phase (Hurrell et al., 2003). Indeed, during negative NAO, their southerly position results in enhanced winter rainfall over the Southern Europe and the NW Mediterranean Sea while under positive NAO, storm trajectory are more northeastwards and precipitation more intense in Northern Europe. Changes in the mid-latitude atmospheric circulation in the North Atlantic is thus expected to impact of the Rhone River flow over the course of the Holocene.

Both a gravity core (KSGC-31) and multi-core (GolHo-1B) were retrieved from virtually the same site in the Rhone mud belt deposited onto the Gulf of Lions inner-shelf (43°0′23″ N; 3°17′56″ E, water depth 60 m) (Fig. 1). The 7 m long gravity core KSGC-31 was recovered during the GM02-Carnac cruise in 2002 on the R/V *Le Suroît*, while the 20 cm long multi-core GolHo-1B was collected during the GolHo cruise in 2013, on the R/V *Nerys*. Both sediment cores were sliced continuously at a sampling step of 1 cm for biomarker analyses.

2.2 Core chronology

The age model of the gravity core KSGC-31 is based on 21 radiocarbon dates obtained by Accelerator Mass Spectrometry (AMS) performed by the Laboratoire de

Mesure du Carbone 14 (Saclay, France) and in the Beta Analytic Radiocarbon Dating Laboratory (Florida, USA) (Table 1). Note that the two uppermost dates indicate post-bomb values. The ^{14}C dates were converted into 1σ calendar years using Calib7.1 (Stuiver and Reimer, 1993) and the MARINE 13 calibration dataset (Reimer et al., 2013) (Table 1). We used a marine reservoir age correction of $\Delta R = 23 \pm 71$ yr (http://calib.qub.ac.uk/marine/regioncalc.php). The age model was obtained by linear interpolation between ^{14}C dates excluding the minor reversal at 18.5 cm (350 ± 78 yr). The age control for the upper portion of the core is based on ^{210}Pb profile measured in the upper 20 cm of KSGC-31 spliced with the ^{210}Pb profile of the GolHo-1B core. Based on the ^{210}Pb chronology, the age of the gravity KSGC-31 core-top was estimated to be approx. 1971 ± 1.4 yr AD. The GolHo-1B core, spanning a range from 1960 ± 5.6 to 2013 yr AD, thus extends the SST record to present day. The two upper post-bomb radiocarbon ages converted using OxCal 4.2 (Ramsey and Lee, 2013) are in good agreement with the ^{210}Pb chronology (Table 1). Details on the establishment of the age model for the past 2000 yr, including splicing of GolHo-1B and upper part of KSGC-31 records can be found in Sicre et al. (2015). The obtained spliced KSGC-31_GolHo-1B SST signal presented here covers the past 10 000 yr, including the 20th century. The mean sedimentation rate is ~ 80 cm $(1000\,\text{yr})^{-1}$.

2.3 Biomarker analyses

Lipids were extracted from 2 to 3 grams of freeze-dried sediments using a mixture of (3 : 1 v/v) dichloromethane/methanol. Alkenones and n-alkanes were isolated for the total lipid extract by silica gel chromatography and quantified by gas chromatography as described by Ternois et al. (1996). The global calibration published by Conte et al. (2006) was used to convert the unsaturation ratio of C_{37} alkenones ($U_{37}^{k'} = C_{37:2}/(C_{37:2}+C_{37:3})$) to SSTs ($T$ (°C) $= -0.957 + 54.293(U_{37}^{k'}) - 52.894(U_{37}^{k'})^2 + 28.321(U_{37}^{k'})^3$). External precision using this calibration has been estimated to be ±1.2 °C while analytical precision after triplicate injections is less than 0.01 $U^{k'}_{37}$ unit ratio, which, in the temperature range of our data, translates into ±0.3 °C.

N-alkane concentrations were calculated using 5α-cholestane as an external standard. Only the high-molecular-weight *n*-alkanes with an odd carbon number, i.e. $C_{27}+C_{29}+C_{31}+C_{33}$ homologs (hereafter TERR-alkanes), were quantified to track land-derived inputs. These compounds are primarily synthesized by higher plants and are constituents of epicuticular waxes of leaves. Their accumulation in the sediments of Gulf of Lions is primarily associated with the discharge and deposition of the Rhone River suspended particles in relation with precipitations (Ludwig et al., 2010).

3 Results

Figure 2a shows the temporal evolution of SSTs at the KSGC-31_GolHo-1B site over the past 10 000 yr, including the post-industrial period. The data indicate warm Early Holocene values, 18 ± 0.4 °C, followed by a long-term cooling starting ~ 7000 yr BP culminating during the Dark Ages (DA), and a Late Holocene warming that do not reach values as high as those of the Early Holocene. Several multi-decadal to century scale cold relapses (CRs) with SSTs were colder by ~ 1 °C (grey bars in Fig. 2) are superimposed to these trends.

TERR-alkanes are used to identify terrestrial inputs from the Rhone River and their possible link to flood events and large-scale precipitation patterns (Fig. 2c). Concentrations range from 300 to 1800 ng g^{-1} with lowest values during early- to mid-Holocene increasing from ~ 7000 yr BP to present, except for a pronounced drop centered ~ 2500 BP. They also show large multi-decadal fluctuations mostly during the second half of the Holocene with highest values during the Common Era (past 2000 yr), maximizing during the Medieval Climate Anomaly (MCA; 900–1300 yr AD), and a decrease over the last century.

In the following section we compare our SST record to earlier published time series from the Western and Eastern Mediterranean basins. We also discuss the Gulf of Lions TERR-alkane record in relation with flood reconstructions from the Northern and Southern Alps (Wirth et al., 2013) and Bourget Lake sediments located in the Upper Rhone River catchment basin (Arnaud et al., 2012) to infer additional information on atmospheric circulation regime.

4 Discussion

4.1 General trends

The temporal evolution of SSTs in the Gulf of Lions depicts three main phases. A warm Early Holocene at the time of high summer insolation in the Northern Hemisphere, ending by a first cold event, CR1 (7000–6000 BP). Thereafter, SSTs show a general decline till about 1000 BP with notable cold intervals (CR2 to CR6) and a final warming over the past century. These main phases have been described by Nesje and Dahl (1993) in the North Atlantic as the Preboreal, Hypsithermal and Neoglacial chronozones. Our record shows strong similarities with the recent world-wide compilation of 73 marine records of Marcott et al. (2013) exhibiting a warm plateau between 10 000 and 5000 yr BP and a 0.7 °C cooling from 5500 to 100 yr BP in the extratropical Northern Hemisphere (30 to 90° N). The 2.5 °C cooling calculated from our record between 7000 and 100 yr BP is similar as the 2 °C calculated by Marcott et al. (2013) in the high-latitude North Atlantic, outlying the influence of the Atlantic climate on the Mediterranean SSTs. Note that cooling in the Gulf of Lions is steeper (~ 3 °C) when calculated from 7000 to 1000 BP.

Figure 3 compares our results with Mediterranean SST published reconstructions (Table 2). Except for the MD99-2343 (δ^{18}O of *G. bulloïdes*) and GeoB7702-3 cores (TEX86) (Castaneda et al., 2010), these reconstructions are all based on alkenone paleothermometry. Owing to age uncertainties and low temporal resolution of these records, only trends and centennial to millennial-scale variability of the climate signals are retained and will be discussed here. Comparison with these regional time-series highlights differences between the Western and Eastern Mediterranean basins.

In particular, the Alboran, Balearic Islands, Gulf of Lions records all show a marked cooling trend through the middle to late Holocene. This is also the case in the central Mediterranean (Adriatic, Southern Tyrrhenian and Ionian seas), while SSTs in the Levantine basin indicate no or slight warming, in agreement with earlier findings of Rimbu et al. (2003). This W–E evolution of Holocene SSTs suggests common features of the mid-latitude North Atlantic and NW Mediterranean that are distinct from the SE Mediterranean.

4.2 North-western Mediterranean CRs

Six CRs of different duration and amplitude were identified in Gulf of Lions SST record. The occurrence of CRs has been previously described in global compilations (Mayewski et al., 2004; Wanner et al., 2011) and seems to be associated with glacier advances in Europe (Denton and Karlén, 1973). They reflect either polar cooling or tropical aridity and likely express atmospheric circulation changes (Mayewski et al., 2004). The influence of the AMV has also been suggested (Kushnir and Stein, 2010). There are, however, discrepancies on the spatio-temporal distribution and amplitude of these events (Wanner et al., 2011, 2014). Each CR does not necessarily impact everywhere with the same intensity due to local responses to climate changes. The sensitivity of proxies or particular sediment settings (e.g. coastal areas), their seasonal character, may also be another reason for not detecting CRs in all records. For example, it is interesting to note that the 8200 yr BP, well expressed in Greenland ice cores, is not found in the core KSGC-31 despite the high temporal resolution of this record. When present in the extratropics, these short-term cooling have been attributed to strong cold and dry winds blowing from the North possibly triggered by a slowdown of the thermohaline circulation in the North Atlantic (Mayewski et al., 2004). According to Kushnir and Stein (2010), cold SSTs in the tropical Atlantic would cause the formation of a high-pressure over the Eastern Atlantic extending towards Western Europe and the W-Mediterranean Sea similar to EA. This large-scale atmospheric pattern would impact on T and precipitations in the Mediterranean region as far as in the Levant region.

Intensified northerly winds during the CR thus likely reinforced convection in the Gulf of Lions by surface cooling (Schroeder et al., 2008; Josey et al., 2011). The study of the Minorca drift sediment (MD99-2343 core, Frigola et al., 2007) suggest that grain size in this area provides a record of bottom current vigor presumably induced by deep-water convection in the Gulf of Lions. To address this issue, we compared the % of non-carbonate fraction $> 10\,\mu$m (UP10) of the Minorca core to our SST reconstruction. As can be seen from Fig. 2a and b most of the CRs of the Gulf of Lions seems to correspond to higher values of UP10. This is less obvious for shorter events when age model uncertainties become limiting for definite conclusions. Synchronicity between episodes of intensified upwelling in the Alboran Sea and high UP10 values at Minorca has also been discussed by Ausin et al. (2015) and explained by NAO. Based on the good match between UP10 values and the NAO index reconstruction of Olsen et al. (2012), these authors put forwards the hypothesis that persistent negative NAO would have triggered both stronger upwelling in the Alboran Sea and northerly or north-westerly winds over the Gulf of Lions, thereby enhancing convection. Extreme cold wind conditions could also result from EA in particular during solar minima (Moffa-Sanchez et al., 2014; Sicre et al., 2015). It is notable that M8 does not show cooling in our record and that Early Holocene SSTs do not fluctuate much till about 7000 yr BP. The density of sub-surface waters also plays a role in the convection process. High heat and salt contents of the LIW underlying surface waters in the Gulf of Lions can act as a pre-conditioning factor to enhance convection (Schroeder et al., 2010). Considering that during the African Humid Period (AHP) (9000–7500 yr BP), the LIW formation in the Eastern Mediterranean was much reduced or shutdown, we speculate that lower amounts of LIW formation during the AHP could have decreased advection of salt in the Gulf of Lions thereby contributing to weaken convection at a time when SSTs are among the warmest in our record due to high summer insolation in the Northern Hemisphere. Lower subsurface salinity waters in the Gulf of Lions could have counter-acted surface atmospheric forcing (heat loss) and caused a reduction of the thermohaline circulation in the Mediterranean Sea during this time period.

4.3 Holocene flood activity

Heavy rain episodes frequently occur in fall in the Western Europe – Mediterranean region resulting in intense floods that can cause important damages. The Alps region is one of the rainiest regions of W-Europe. Most of the precipitations occur in autumn and contribute through various tributaries to the water discharge of the Rhone River. The catchment area of the upper Rhone River receives precipitations originating from the North Atlantic along the year, and from the Southern Lower Rhone tributaries during extreme rainfalls occurring in September and October. As a result the water and solid discharges of the Rhone River in the NW-Mediterranean Sea is highly seasonal. About 80% of the sediments of the Gulf of Lions continental shelf is supplied by the Rhone River (Aloïsi et al., 1977).

We compared our record of TERR-alkanes to two regional reconstructions of flood intensity of the Northern and Southern Alps obtained from 15 lacustrine sediment cores (Wirth et al., 2013). As can be seen from Fig. 4, TERR-alkanes in KSGC-31_GolHo-1B share some resemblance with the flood intensity of the N-Alps. Notably, lowest values between 10 000 and 7000 yr BP and low hydrological activity in Lake Bourget (Arnaud et al., 2012) between 10 000 and 6000 yr BP agrees with lower TERR-alkanes (Fig. 4c). This result has been attributed to melting of the Rhone Glacier due to high summer insolation (Goehring et al., 2011). During the past 6000 yr, these three records show a tendency to more floods with larger fluctuations, in particular during the last millennium. High TERR-alkanes and N-Alps flood activity coincide with phases of glacier advances (Wirth et al., 2013) and sediment flux increase in the Rhone delta plain (Provansal et al., 2003; Fanget et al., 2014). Similar trends of TERR-alkanes and N-Alps flood activities suggest that the suspended particles deposited in the Gulf of Lions originate primarily from the Upper Rhone River. Comparison of TERR-alkane and flood activity in the N-Alps with NAO (Fig. 4d) indicates that high values occur during positive NAO.

Flood activity from the S-Alps differs from the other two flood reconstructions mainly during the Early Holocene and between 4200 and 2400 yr BP. Higher flood activity during the latter period coincides with extreme negative NAO values. Under such conditions storminess is enhanced in the Mediterranean. The concomitance of the most intense flood of the S-Alps ~ 2400 yr with cold SSTs and high UP10 emphasize extreme conditions during most negative NAO. The TERR-alkane drastic decline is consistent with lower precipitation in the upper Rhone river catchment basin (Fig. 2). As discussed by Fanget et al. (2014), flood activity and changes in Rhone River discharge during the Common Era result from both climate conditions and human activity, i.e. erosion due to land use.

5 Conclusions

Alkenone-derived SSTs from core KSGC-31_GolHo-1B provide a regional reconstruction of Holocene climate variability of the NW Mediterranean. After a warm plateau between 10 000 and 7000 yr BP, SSTs depict a cooling trend of 2.5 °C from 7000 to 100 yr, comparable to the North Atlantic, primarily as a result of orbital forcing. The Late Holocene warming reversed this long-term cooling trend. Six CRs of different duration and amplitude were identified, with the notable exception for the 8200 yr event. Northerly and northwesterly winds blowing over the Gulf of Lions during negative NAO, and/or EA, are the most likely cause of these cold events.

Comparison of TERR-alkanes accumulated in the inner shelf of the Gulf of Lions with records of flood intensity from the Alps indicates that they primarily originate from the Upper Rhone River catchment basin and are delivered during positive NAO. The several century-long lowest levels of TERR-alkanes centered ~ 2500 yr coincide with a period of persistent negative NAO. Our results highlight the influence of the mid-latitude atmospheric circulation on the NW Mediterranean SSTs and precipitations on decadal to multi-decadal time scales over the Holocene.

Acknowledgements. We would like to thank MISTRALS/Paleomex for financial support and the crew operating the GMO2 Carnac (R/V *Le Suroît*) and GolHo (R/V *Nerys*) cruises. Nabil Sultan (GMO2 Carnac Chief Scientist) Serge Berné (IFREMER-CEFREM) and Bernard Dennielou (IFREMER) are thanked for giving access to the core KSGC-31 and to IFREMER laboratory facilities. The ARTEMIS programme is thanked for providing 14C from the Accelerator Mass Spectrometer located in Saclay, France (Laboratoire de Mesure du 14C).

References

Aloïsi, J. C., Auffret, G. A., Auffret, J. P., Barusseau, J. P., Hommeril, P., Larsonneur, C., Monaco, A.: Essai de modélisation de la sédimentation actuelle sur les plateaux continentaux français, B. Soc. Geol. Fr., 19, 183–195, 1977.

Arnaud, F., Révillon, S., Debret, M., Revel, M., Chapron, E., Jacob, J., Giguet-Covex, C., Poulenard, J., and Magny, M.: Lake Bourget regional erosion patterns reconstruction reveals Holocene NW European Alps soil evolution and paleohydrology, Quaternary Sci. Rev., 51, 81–92, doi:10.1016/j.quascirev.2012.07.025, 2012.

Auclair, F., Marsaleix, P., and Estournel, C.: Sigma coordinate pressure gradient errors: evaluation and reduction by an inverse method, J. Atmos. Ocean. Tech., 17, 1348–1367, 2000.

Ausín, B., Flores, J. A., Sierro, F. J., Cacho, I., Hernández-Almeida, I., Martrat, B., and Grimalt, J. O.: Atmospheric patterns driving Holocene productivity in the Alboran Sea (Western Mediterranean): a multiproxy approach, The Holocene, 25, 1–13, doi:10.1177/0959683614565952, 2015.

Bassetti, M. A., Berné, S., Fontanier, C., Buscail, R., Sicre, M. A., Dennielou, B., and Jouet, G.: Holocene hydrological changes of the Rhone river as recoded in the marine mud belt, Clim. Past, in preparation, 2015.

Brown, M.: Ocean Data View 4.0, Oceanography, 11, 19–21, 1998.

Cacho, I., Grimalt, J. O., Canals, M., Sbaffi, L., Shackleton, N., Schönfeld, J., and Zahn, R.: Variability of the western Mediterranean Sea surface temperature during the last 25 000 years and its connection with the Northern Hemisphere climatic changes, Paleoceanography, 16, 40–52, 2001.

Castañeda, I. S., Schefuß, E., Pätzold, J., Sinninghe Damsté, J. S., Weldeab, S., and Schouten, S.: Millennial-scale sea surface temperature changes in the eastern Mediterranean (Nile River Delta region) over the last 27 000 years, Paleoceanography, 25, PA1208, doi:10.1029/2009PA001740, 2010.

Cattaneo, A. and Steel, R. J.: Transgressive deposits: a review of their variability, Earth-Sci. Rev., 62, 187–228, 2003.

Conte, M. H., Sicre, M.-A., Rühlemann, C., Weber, J. C., Schulte, S., Schulz-Bull, D., and Blanz, T.: Global temperature calibration of the alkenone unsaturation index (UK37) in surface waters and comparison with surface sediments, Geochem. Geophy. Geosy., 7, Q02005, doi:10.1029/2005GC001054, 2006.

Denton, G. H. and Karlen, W.: Holocene climatic variations their pattern and possible cause, Quaternary Res., 3, 155–205, 1973.

Emeis, K.-C., Struck, U., Schulz, H.-M., Bernasconi, S., Sakamoto, T., and Martinez-Ruiz, F.: Temperature and salinity of Mediterranean Sea surface waters over the last 16,000 years: constraints on the physical environment of S1 sapropel formation based on stable oxygen isotopes and alkenone unsaturation ratios, Palaeogeogr. Palaeocl., 158, 259–280, 2000.

Emeis, K. C., Struck, U., Blanz, T., Kohly, A., and Woß, M.: Salinity changes in the central Baltic Sea (NW Europe) over the last 10 000 years, The Holocene 13, 411–421, 2003.

Essallami, L., Sicre, M.-A., Kallel, N., Labeyrie, L., and Siani, G.: Hydrological changes in the Mediterranean Sea over the last 30 000 years, Geochem. Geophy. Geosy., 8, Q07002, doi:10.1029/2007GC001587, 2007.

Fanget, A. S., Berné, S., Jouet, G., Bassetti, M.-A., Dennielou, B., Maillet, G. M., and Tondut, M.: Impact of relative sea level and rapid climate changes on the architecture and lithofacies of the Holocene Rhone subaqueous delta (Western Mediterranean Sea), Sediment. Geol., 305, 35–53, doi:10.1016/j.sedgeo.2014.02.004, 2014.

Frigola, J., Moreno, A., Cacho, I., Sierro, F. J., Flores, J. A., Grimalt, J. O., Hodell, D. A., and Curtis, J. H.: Holocene climate variability in the western Mediterranean region from a deepwater sediment record, Paleoceanography, 22, PA2209, doi:10.1029/2006PA001307, 2007.

Giunta, S., Emeis, K. C., and Negri, A.: Sea-surface temperature reconstruction of the last 16 000 years in the Eastern Mediterranean Sea, Rivista Italiana di Paleontologia e Stratigrafia, 107, 463–476, 2001.

Goehring, B. M., Schaefer, J. M., Schluechter, C., Lifton, N. A., Finkel, R. C., Jull, A. J. T., Akçar, N., and Alley, R. B.: The Rhone Glacier was smaller than today for most of the Holocene, Geology, 39, 679–682, 2011.

Hurrell, J. W., Kushnir, Y., Ottersen, G., and Visbeck, M.: An overview of the North Atlantic Oscillation; The North Atlantic oscillation: climate significance and environmental impact, Geoph. Monog., 134, 1–35, 2003.

Josey, S. A., Somot, S., and Tsimplis, M.: Impacts of atmospheric modes of variability on Mediterranean Sea surface heat exchange, J. Geophys. Res.-Oceans, 116, C02032, doi:10.1029/2010JC006685, 2011.

Kushnir, Y. and Stein, M.: North Atlantic influence on 19th–20th century rainfall in the Dead Sea watershed, teleconnections with the Sahel, and implication for Holocene climate fluctuations, Quaternary Sci. Rev., 29, 3843–3860, 2010.

Ludwig, W., Bouwman, A. F., Dumont, E., and Lespinas, F.: Water and nutrient fluxes from major Mediterranean and Black Sea rivers: past and future trends and their implications for the basin scale budgets, Global Biogeochem. Cy., 24, GB0A13, doi:10.1029/2009GB003594, 2010.

Marcott, S. A., Shakun, J. D., Clark, P. U., and Mix, A. C.: A reconstruction of regional and global temperature for the past 11 300 years, Science, 339, 1198–1201, 2013.

Martrat, B., Jimenez-Amat, P., Zahn, R., and Grimalt, J.-O.: Similarities and dissimilarities between the last two deglaciations and interglaciations in the North Atlantic region, Quaternary Sci. Rev., 99, 122–134, doi:10.1016/j.quascirev.2014.06.016, 2014.

Mayewski, P. A., Rohling, E. E., Stager, J. C., Karlen, W., Maasch, K. A., Meeker, L. D., Meyerson, E. A., Gasse, F., van Kreveld, S., Holmgren, K., Lee-Thorp, J., Rosqvist, G., Rack, F., Staubwasser, M., Schneider, R. R., and Steig, E. J.: Holocene climate variability, Quaternary Res., 62, 243–255, 2004.

Millot, C.: The Gulf of Lions' hydrodynamics, Cont. Shelf. Res., 10, 885–894, 1990.

Millot, C.: Circulation in the Western Mediterranean Sea, J. Marine Syst., 20, 423–442, 1999.

Müller, P. J., Kirst, G., Ruthland, G., von Storch, I., and Rosell-Melé, A.: Calibration of the alkenone paleotemperature index UK'37 based on core-tops from the eastern South Atlantic and the global ocean (60 N-60 S), Geochim. Cosmochim. Ac., 62, 1757–1772, 1998.

Moffa-Sanchez, P., Born, A., Hall, I. R., Thornalley, D. J. R., and Barker, S.: Solar forcing of North Atlantic surface temperature and salinity over the past millennium, Nat. Geosci., 7, 275–278, 2014.

Nesje, A. and Dahl, S. O.: Late glacial and Holocene glacier fluctuations and climate variations in Western Norway: a review, Quaternary Sci. Rev., 12, 255–261, 1993.

Olsen, J., Anderson, N. J., and Knudsen, M. F.: Variability of the North Atlantic Oscillation over the past 5200 years, Nat. Geosci., 5, 808–812, 2012.

Provansal, M., Vella, C., Arnaud-Fassetta, G., Sabatier, F., and Maillet, G.: Role of fluvial sediment inputs in the mobility of the Rhône delta coast (France), Geomorphologie, 4, 271–282, 2003.

Ramsey, C.-B. and Lee, S.: Recent and planned developments of the program OxCal, Radiocarbon, 55, 720–730, 2013.

Reimer, P. J., Bard, E., Bayliss, A., Beck, J. W., Blackwell, P. G., Bronk Ramsey, C., Grootes, P. M., Guilderson, T. P., Haflidason, H., Hajdas, I., HattŽ, C., Heaton, T. J., Hoffmann, D. L., Hogg, A. G., Hughen, K. A., Kaiser, K. F., Kromer, B., Manning, S. W., Niu, M., Reimer, R. W., Richards, D. A., Scott, E. M., Southon, J. R., Staff, R. A., Turney, C. S. M., and van der Plicht, J.: IntCal13 and Marine13 Radiocarbon Age Calibration Curves 0–50 000 years cal BP, Radiocarbon, 55, 1869–1887, 2013.

Rimbu, N., Lohmann, G., Kim, J.-H, Arz, H. W., and Schneider, R.: Arctic/North Atlantic oscillation signature in holocene sea surface temperature trends as obtained from alkenone data, Geophys. Res. Lett., 30, 1280, doi:10.1029/2002GL016570, 2003.

Rohling, E. J., Mayewski, P. A., Abu-Zied, R. H., Casford, J. S. L., and Hayes, A.: Holocene atmosphere–ocean interactions: records from Greenland and the Aegean Sea, Clim. Dynam., 18, 587–593, doi:10.1007/s00382-001-0194-8, 2002.

Schroeder, K., Borghini, M., Cerrati, G., Difesca, V., Delfanti, R., Santinelli, C., and Gasparini, G. P.: Multiparametric mixing analysis of the deep waters in the western Mediterranean Sea, Chem. Ecol., 24, 47–56, 2008.

Schroeder, K., Josey, S. A., Herrmann, M., Grignon, L., Gasparini, G. P., and Bryden, H. L.: Abrupt warming and salting of the Western Mediterranean Deep Water after 2005: atmospheric forcings and lateral advection, J. Geophys. Res., 115, C08029, doi:10.1029/2009JC005749, 2010.

Schroeder, K., Haza, A. C., Griffa, A., Özgökmen, T. M., Poulain, P., Gerin, R., Peggion, G., and Rixen, M.: Relative dispersion in the liguro-provencal basin: from sub-mesoscale to mesoscale, Deep-Sea Res. Pt. I, 58, 861–882, 2011.

Sicre, M.-A., Martrat, B., Jalali, B., Schmidt, S., Bassetti, M.-A., and Kallel, N.: Sea surface temperature variability in the North Western Mediterranean Sea (Gulf of Lions) during the Common Era, Earth Planet. Sc. Lett., revised, 2015.

Stuiver, M. and Reimer, P. J.: Extended ^{14}C database and revised CALIB 3.0 ^{14}C age calibration program, Radiocarbon, 35, 215–230, 1993.

Ternois, Y., Sicre, M.-A., Boireau, A., Marty, J.-C., and Miquel, J.-C.: Production pattern of alkenones in the Mediterranean Sea, Geophys. Res. Lett., 23, 3171–3174, 1996.

Trouet, V., Esper, J., Graham, N. E., Baker, A., Scourse, J. D., and Frank, D. C.: Persistent positive North Atlantic oscillation mode dominated the medieval climate anomaly, Science, 324, 78–80, 2009.

Wanner, H., Solomina, O., Grosjean, M., Ritz, S. P., and Jetel, M.: Structure and origin of Holocene cold events, Quaternary Sci. Rev., 30, 3109–3123, 2011.

Wanner, H., Mercolli, L., Grosjean, M., and Ritz, S. P.: Holocene climate variability and change; a data-based review, J. Geol. Soc. London, 172, 254–263, doi:10.1144/jgs2013-101, 2014.

Wirth, S. B., Glur, L., Gilli, A., and Anselmetti, F. S.: Holocene flood frequency across the Central Alps – solar forcing and evidence for variations in North Atlantic atmospheric circulation, Quaternary Sci. Rev., 80, 112–128, doi:10.1016/j.quascirev.2013.09.002, 2013.

Table 1. AMS radiocarbon dated levels and their calibrated ages with a 1σ uncertainty for the KSGC-31 gravity core. The analyses were performed at the Laboratoire de Mesure du Carbone 14, Saclay (France) and at the Beta Analytic Radiocarbon Dating Laboratory (Florida; USA). Raw radiocarbon ^{14}C ages were corrected and calibrated to calendar ages using the Calib7.1 software (Stuiver and Reimer, 1993) and the MARINE13 calibration dataset (Reimer et al., 2013).

Depth (cm)	Material	Radiocarbon age ±1σ error (yr BP)	Calibrate Age (cal BP)	±1σ error
5.5	*Bittium* sp.	420 ± 30	24[a]	60
11.5	*Tellina* sp.	430 ± 30	34[a]	60
18.5	*Pecten* sp.	720 ± 40	350[b]	78
25.5	*Venus* sp.	640 ± 30	234	99
41	*Pecten* sp.	700 ± 30	339	79
52	Indet. bivalve	960 ± 30	551	59
71	*Arca tetragona*	1340 ± 30	851	80
110.5	*Venus* sp.	1465 ± 30	992	85
186.5	*Nucula* sp.	2235 ± 40	1805	99
251	Juvenile bivalve shells (ind.)	2940 ± 30	2674	100
330.5	Venus cosina	3870 ± 30	3796	106
370.5	Nuculana sp.	4170 ± 30	4223	113
390.5	Turritella sp.	4500 ± 30	4676	106
460	Venus sp.	5530 ± 45	5873	106
481	Ostrea sp	5955 ± 35	6348	78
501.5	Turritella sp.	6380 ± 50	6826	107
552	coquilles	7215 ± 30	7653	75
583	Turritella sp.	7860 ± 60	8288	92
652	Turritella sp.	8310 ± 35	8843	121
700.5	Turritella sp.	9215 ± 30	10 006	123
701	Turritella sp.	9190 ± 50	9968	145

[a] post-bomb radiocarbon ages, obtained using OxCal 4.2 (Ramsey and Lee, 2013), not used for the interpolation.

[b] Reversal date, not used for the interpolation.

Table 2. List of data sets used in Fig. 3.

Location/Core	Proxy	Temperature Calibration/ Reference	Latitude (°)	Longitude (°)	Elevation (m)	Resolution (yr)	Reference
ODP Site 161–976	UK’37	Müller et al. (1998)	30.20	−4.31	−1108	34	Martrat et al. (2014)
MD95-2043	UK’37	Müller et al. (1998)	36.10	−2.60	−1000	110	Cacho et al. (2001)
KSGC-31_GolHo-1B	UK’37	Conte et al. (2006)	43.00	3.29	−60	14	This study
MD99-2343	δ^{18}O (G. bulloides)	–	40.49	4.02	−2391	110	Frigola et al. (2007)
BS79-38	UK’37	Müller et al. (1998)	38.41	13.57	−1489	59	Cacho et al. (2001)
AD91-17	UK’37	Müller et al. (1998)	40.90	18.60	−844	190	Giunta et al. (2001)
M25/4-KL11	UK’37	Müller et al. (1998)	36.70	17.70	−3376	260	Emeis et al. (2003)
M40/4-SL78	UK’37	Müller et al. (1998)	37.03	13.18	−467	160	Emeis et al. (2003)
MD 99-917	UK’37	Conte et al. (2006	41.28	17.61	−1010	40	Essallami et al. (2007)
GeoB 7702-3	TEX86 UK’37	Kim et al. (2008) Müller et al. (1998)	31.7	34.1	−562	210	Castañeda et al. (2010)
ODP Site 160-967D	UK’37	Müller et al. (1998)	34.07	32.72	−2552	94	Emeis et al. (2000)
LC21	Warm foram species (%)	–	35.67	26.58	−1522	125	Rohling et al. (2002)

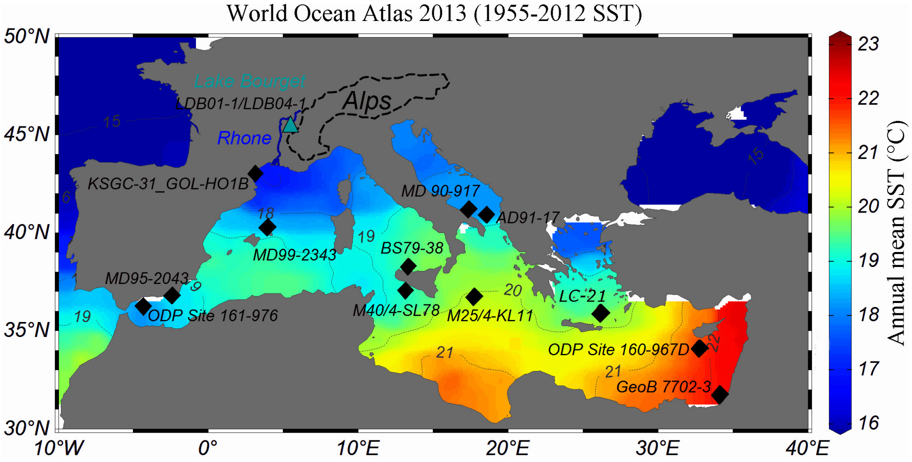

Figure 1. Map of the Mediterranean annual mean SSTs (°C) (1955 and 2012) from Word Ocean Atlas 2013 (http://odv.awi.de/de/data/ocean/world_ocean_atlas_2013/) plotted using Ocean Data View (Brown, 1998). The location of the KSGC-31_GolHo-1B core and other sites discussed in the text are also reported (from West to East): ODP Site 161–976, Alboran Sea (Martrat et al., 2014); MD95-2043, Alboran Sea (Cacho et al., 2001); MD 99-2343, Balearic basin (Frigola et al., 2007); M40/4-SL78, Ionian Sea (Emeis et al., 2003); BS79-38, Southern Tyrrhenian Sea (Cacho et al., 2001); MD90-917, Southern Adriatic Sea (Essallami et al., 2007); M25/4-KL11, the Ionian Sea (Emeis et al., 2003); AD91-17, Southern Adriatic Sea (Giunta et al., 2001); LC-21, Aegean Sea (Rohling et al., 2002); ODP Site 160-967D, Levantine basin (Emeis et al., 2000); GeoB 7702-3, Levantine basin (Castaneda et al., 2010) and LDB01-1 and LDB04-1. The location of Lake Bourget in France is also shown (Arnaud et al., 2012).

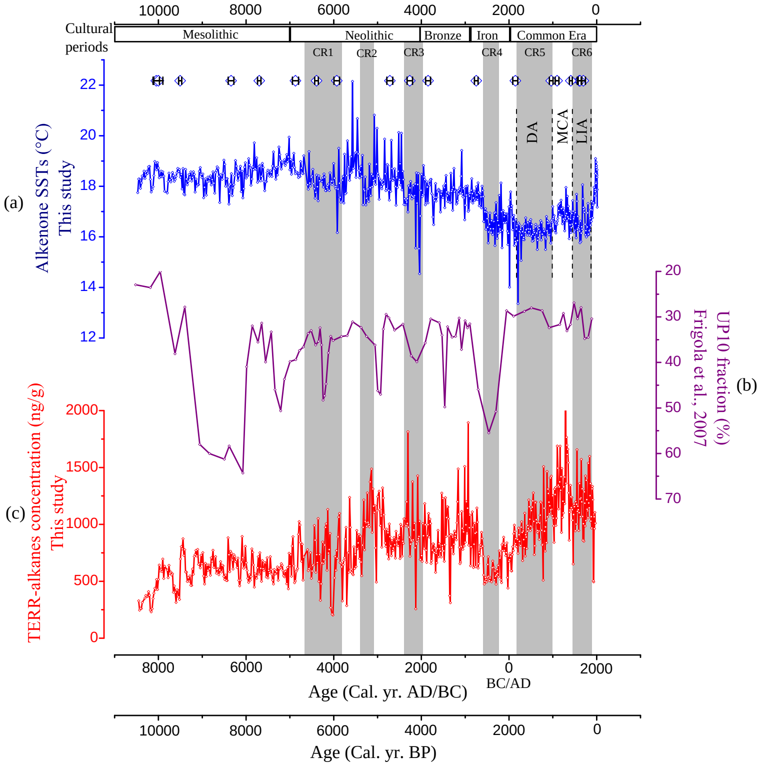

Figure 2. Alkenone SSTs and TERR-alkane concentrations at the KSGC-31_GolHo-1B core site over the past 10 000 yr. **(a)** The AMS ^{14}C radiocarbon dates for gravity core KSGC-31 are indicated by the blue diamonds; vertical dashed lines highlight the major periods of the Common Era. **(b)** The UP10 fraction from core MD99-2343 (Frigola et al., 2007), (reversed vertical axis). **(c)** TERR-alkane concentrations. The vertical gray bars represent the six NW Mediterranean CRs no. 1–6 (Wanner et al., 2014).

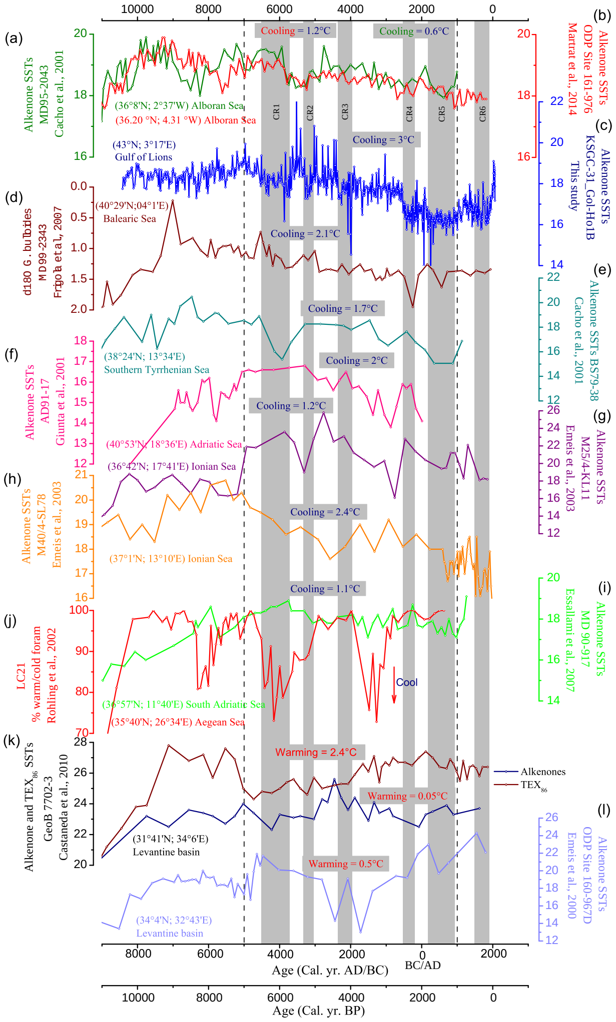

CPD

11, 3187–3209, 2015

Holocene climate variability in the North-Western Mediterranean Sea (Gulf of Lions)

B. Jalali et al.

Title Page
Abstract
Introduction
Conclusions
References
Tables
Figures
◂◂
▸▸
◂
▸
Back
Close
Full Screen / Esc
Printer-friendly Version
Interactive Discussion

Figure 3. SST records in the Mediterranean Sea over the Holocene. **(a)** Core MD95-2043 from the Alboran Sea (Cacho et al., 2001). **(b)** ODP Site 161–976 from the Alboran Sea (Martrat et al., 2014). **(c)** Core KSGC-31_GolHo-1B from the Gulf of Lions (this study). **(d)** G. bulloides oxygen isotopic record for core MD99-2343 from the Balearic Sea (Frigola et al., 2007). **(e)** Core BS79-38 from the Southern Tyrrhenian Sea (Cacho et al., 2001). **(f)** Core AD91-17 from the Adriatic Sea (Giunta et al., 2001). **(g)** Core M25/4-KL11 from the Ionian Sea (Emeis et al., 2003). **(h)** Core M40/4-SL78 from the Ionian Sea (Emeis et al., 2003). **(i)** Core MD90-917 from the Southern Adriatic Sea (Essallami et al., 2007). **(j)** Core LC-21 from the Aegean Sea (Rohling et al., 2002). **(k)** Core GeoB 7702-3 from the Levantine basin (Castaneda et al., 2010). **(l)** ODP Site 160-967D from the Levantine basin (Emeis et al., 2000). Vertical grey bars represent the time interval of the CRs, no. 1–6. The grey vertical dashed lines indicate the time interval used to calculate SST trends (7000 to 1000 yr BP).

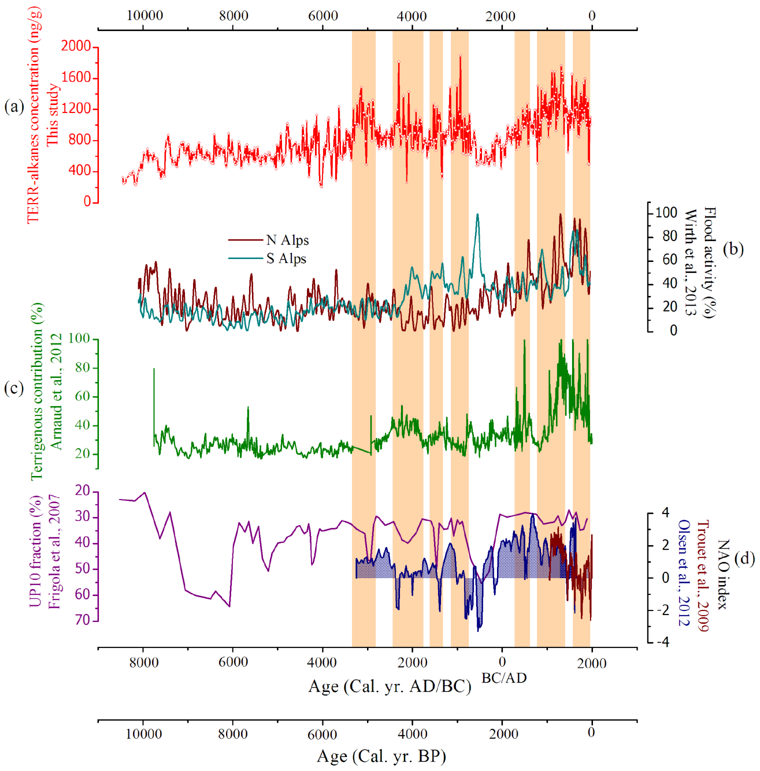

Figure 4. Holocene flood changes in the NW Mediterranean Sea and Alps region. **(a)** TERR-alkane abundances as a proxy of flood intensity. **(b)** Flood activity in the North and South Alps (from Wirth et al., 2013). **(c)** Total terrigenous fraction (%) indicates the Rhone river discharge into lake Bourget (Arnaud et al., 2012) (green curve). **(d)** The UP10 fraction from core MD99-2343 (Frigola et al., 2007) (purple curve) and the winter-NAO index from Trouet et al. (2009) (in red) and Olsen et al. (2012) (blue). Vertical light brown bars indicate the periods of high flood intensity based on the high TERR-alkane peaks.